



ARTICLE

## An Effective Lung Cancer Diagnosis Model Using Pre-Trained CNNs

Majdi Rawashdeh<sup>1,2,\*</sup>, Muath A. Obaidat<sup>3</sup>, Meryem Abouali<sup>4</sup>, Dhia Eddine Salhi<sup>5</sup> and Kutub Thakur<sup>6</sup>

<sup>1</sup>Department of Business Information Technology, Princess Sumaya University for Technology, Amman, 11941, Jordan

<sup>2</sup>Department of Computer Engineering, Al Yamamah University, Riyadh, 11512, Saudi Arabia

<sup>3</sup>Department of Computer Science, John Jay College and the Graduate Center, The City University of New York, New York, NY 10019, USA

<sup>4</sup>Department of Computer Science, John Jay College at the City University of New York, New York, NY 10019, USA

<sup>5</sup>LIMOSE Laboratory, Department of Computer Science, M'hamed Bougara University, Boumerdes, 35000, Algeria

<sup>6</sup>Department of Professional Security Studies, New Jersey City University, Jersey City, NJ 07305, USA

\*Corresponding Author: Majdi Rawashdeh. Email: m.rawashdeh@psut.edu.jo

Received: 23 January 2025; Accepted: 13 March 2025; Published: 11 April 2025

**ABSTRACT:** Cancer is a formidable and multifaceted disease driven by genetic aberrations and metabolic disruptions. Around 19% of cancer-related deaths worldwide are attributable to lung and colon cancer, which is also the top cause of death worldwide. The malignancy has a terrible 5-year survival rate of 19%. Early diagnosis is critical for improving treatment outcomes and survival rates. The study aims to create a computer-aided diagnosis (CAD) that accurately diagnoses lung disease by classifying histopathological images. It uses a publicly accessible dataset that includes 15,000 images of benign, malignant, and squamous cell carcinomas in the lung. In addition, this research employs multiscale processing to extract relevant image features and conducts a comprehensive comparative analysis using four Convolutional Neural Network (CNN) based on pre-trained models such as AlexNet, VGG (Visual Geometry Group)16, ResNet-50, and VGG19, after hyper-tuning these models by optimizing factors such as batch size, learning rate, and epochs. The proposed (CNN + VGG19) model achieves the highest accuracy of 99.04%. This outstanding performance demonstrates the potential of the CAD system in accurately classifying lung cancer histopathological images. This study contributes significantly to the creation of a more precise CNN-based model for lung cancer identification, giving researchers and medical professionals in this vital sector a useful tool using advanced deep learning techniques and publicly available datasets.

**KEYWORDS:** Lung cancer; machine learning; computer aided diagnosis; CNN; medical imaging; transfer learning

### 1 Introduction

Cell growth, which is not normal in any area of the body, causes the occupation of space and leads to the development of a condition known as cancer. If these unusual cells develop in the lung area, it can result in lung cancer. The World Health Organization (WHO) states that lung cancer is classified as a non-communicable disease, and it is the fifth highest cause of death globally when considering all possible causes, including trachea and bronchus cancer [1]. Over the past few decades, lung cancer has emerged as the most prevalent cancer globally, affecting a significant number of people and resulting in a death rate close to 1.59 million annually. Based on [2], lung cancer is predicted to have the highest incidence of new cases (222,500 cases) among all cancers in the United States in 2017 when taking men and women together, as well as the highest mortality rate (155,870 deaths) for both sexes. It will rank second in terms of



cause of death for both men and women, coming in second only to breast cancer for women and prostate cancer for men [3]. The CNN (Convolutional Neural Network)-based methods used for classifying lung nodules are shown in Fig. 1. Many lives can be saved when cancer cells are diagnosed early. Due to the differences in the morphological patterns of lung tissues, it is challenging to precisely identify every nodule using these methods. Therefore, determining whether a lung nodule is benign or malignant depends on its discovery. The accidental failure in the CT screening process is precisely located using the CAD approach. Even while it can be difficult to accurately predict diseases using human interpretations, it is not always desirable to obtain precise findings since it can occasionally lead to missprophecies. It will be simpler to anticipate the impacted location for system-aided exams. In addition, imaging methods, including magnetic resonance imaging (MRI), CT scans, and X-rays, can be utilized to visualize the affected area. Every method of detection is exposed to radiation, and each has pros and cons of its own. Increased radiation doses have an impact on the body, and decreasing radiation doses result in hazy images. As a result, a thorough method for applying computer diagnostics to human healthcare has emerged. Two primary classification methods used for training and evaluating datasets to meet system requirements are ANN and SVM, which are utilized to improve the accuracy of CAD systems. Based on the findings, SVM classifier efficiency has significantly reduced erroneous rate densities and achieved 97% sensitivity and accuracy when compared to ANN classifiers [4].

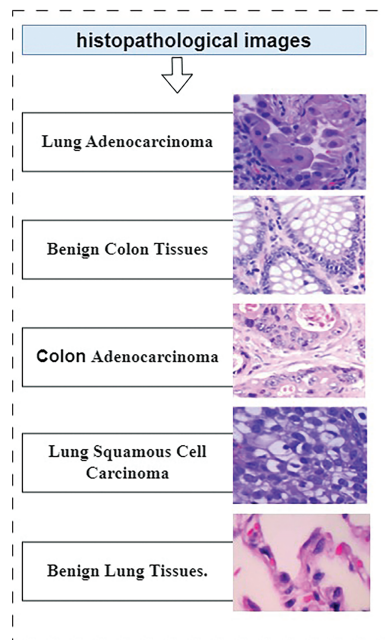


**Figure 1:** Types of cancer in histopathological images

The need for this work is highlighted by the severity and complexity of cancer as a disease, particularly lung cancer, which is among the leading causes of cancer-related deaths worldwide. The 5-year survival rate for lung cancer is alarmingly low at 19%, highlighting the critical importance of early detection in improving treatment outcomes and overall survival. The costs associated with lung nodule screening are high, and because nodules vary widely in size and shape, it can be challenging to identify abnormalities. However, Physicians now depend heavily on computer-aided diagnostic (CAD) technology to help them with this difficult task.

If experiments on machine learning-based digital pathology photo categorization prove fruitful, these technologies can see increased use in pathology clinics. Future predictions indicate a rapid rise in the application of machine learning-based solutions and AI, especially in the field of pathology. Lung cancer is the deadliest kind of disease; however, patients' chances are greatly improved by early detection. Determining whether lung nodules need a biopsy to check for benign or malignant nature is now best achieved through low-dose computed tomography. This method has a somewhat significant risk of false positives in clinical settings. It usually requires many possibly malignant nodules to be identified to perform a biopsy, which leads to a significant number of unnecessary biopsies being performed on individuals who aren't cancer patients.

All acronyms listed in [Table 1](#) reflect the interdisciplinary nature of research in this domain, where lung and colon cancer-based medical imaging techniques converge.

**Table 1:** Below is a compilation of critical acronyms and their full forms

Acronym	Full form
CNN	Convolutional Neural Network
VGG 16/19	Visual Geometry Group (16/19)
ResNet	Residual Neural Network
3D-CNN	3-Dimensional Convolutional Neural Network
CT	Computed Tomography
SVM	Support Vector Machine
SGD	Stochastic Gradient Descent
CAD	Computer Aided Diagnosis
MRI	Magnetic Resonance Imaging
ANN	Artificial Neural Network
WHO	World Health Organization
LIDC	Lung image Database Consortium
IDRI	Image Database Resource Imitative
ILSVRC	ImageNet Large Scale Visual Recognition Challenge
LDCT	Low Dose Computed Tomography
MLP	Multilayer Perceptron
KNN	K-Nearest Neighbor
LUNA16	Lung Nodule Analysis 16
DenseNet	Densely Connected Convolutional Networks
GAN	Generative Adversarial Networks
MFF-CNN	Multi-Scale Feature Fusion Convolutional Neural Network

This study achieves several significant milestones:

- It combines (CNN + VGG19) model for detecting lung and colon cancer, integrating deep feature extraction, high-performance filtering, and ensemble learning strategy, providing an efficient and effective solution.
- It compares and analyzes the performance of pre-trained models (CNN, VGG16, VGG19, ResNet-50, and CNN+VGG19).
- It develops a unique feature extraction technique, using various transfer learning models to extract robust features, enhancing the accuracy of cancer diagnosis.

- It demonstrates the effectiveness of the proposed model lung and colon diagnosis by conducting an extensive evaluation of the LC25000 dataset utilizing an extensive range of metrics, contributing to the advancement of AI-based healthcare applications.

Lastly, the manuscript is organized as follows: [Section 2](#) provides a comprehensive review of existing methods for classifying lung and colon cancer images, highlighting their strengths and weaknesses. [Section 3](#) presents a detailed description of the proposed methodology, including tools and techniques for analyzing cancer images. [Section 4](#) covers results and discussion and provides experimental details, such as parameters and results of the proposed model with metrics and a comparison of existing methods. Finally, [Section 5](#) concludes with a summary of findings and contributions, limitations, potential areas of improvement, and research directions and applications.

## 2 Related Work

CNNs have been used since the late 1980s to address a variety of visual issues. In 1989, LeCun et al. recognized handwritten zip codes using ConvNet, an initial replication approach in multilayered CNN [5,6]. Then, Khehrah et al. [7] reported a technique for finding lung lesions on CT scans that uses shape-based and statistical characteristics. In addition, Lung nodule identification utilizing texture and form characteristics in an artificial neural network was introduced in a different study [8]. The model attained an accuracy of 89.62%. Analogously, a 96.67% accurate model for lung cancer diagnosis based on ANN was proposed by Nasser et al. [9]. A neural network-based lung cancer detection method with 96.67% accuracy using CT images was presented by Mohandass et al. [10]. In addition, LeNet-5 was proposed in 1998 by LeCun et al. [11], an enhanced version of ConvNet, for character classification in documents. In a study done by researchers in reference [12], they used thoracic CT scans to distinguish between malignant pulmonary and benign nodules using the LeNet-5 model. The experimental results were obtained using the datasets from the Image Database Resource Initiative (IDRI) and the Lung Image Database Consortium (LIDC). The model classification was evaluated using a 10-folder cross-validation. The accuracy of the LeNet-5 in differentiating between benign and malignant nodules was 97.041%, and it achieved an accuracy of 96.685% in distinguishing between serious malignancies and mild malignancies. In addition, another study [13] used a hybrid convolutional neural network based on a mix of LeNet and AlexNet to classify lung nodules. The hybrid design made use of both the LeNet layers and the AlexNet parameters. The LIDC-IDRI dataset provided 1018 CT images in total, which were used for the training and evaluation of the agile convolutional neural network. Achieving great accuracy requires careful consideration of several factors, including learning rate, batch size, weight initialization, and kernel size. The framework obtained 0.822 accuracy and 0.877 for the area under the curve (AUC) using  $7 \times 7$  kernel size, 32 batch size, and 0.005 learning rate. In this work, Dropout and Gaussian were also used. In 2012, Sharma et al. released AlexNet [14]. AlexNet won the 2012 ILSVRC, surpassing competitors with a top 5 error rate of 15.3%, demonstrating a widespread advancement in CNN performance. The researchers in [15] proposed two designs for the categorization of pulmonary nodules: hybrid 3D-CNN and straight 3D-CNN. Although the classifiers in the two models were different, the feature extraction technique remained the same. The pulmonary CT images were classified Using the 3D-CNN model's SoftMax classifier, while the hybrid 3D-CNN employed an SVM classifier based on the radial basis function (RBF). The results of the experiment showed that the accuracy of straight 3D-CNN models and the hybrid 3D-CNN was higher. However, when compared to a SoftMax classifier for the 3D-CNN model, the strategy achieved 91.9% precision, 88.53% sensitivity, 94.23% specificity, and 91.8% accuracy.

Ali et al. [16] made use of convolutional neural networks to classify lung tumors. A final fully linked layer, a dropout layer, a pooling layer, and two convolution layers comprise the proposed CanNet architecture. The accuracy achieved by artificial neural networks was 72.50%, while LeNet achieved an accuracy of

56.0%, and CanNet achieved an accuracy of 76.00%. Compared to the LeNet and ANN networks, the CanNet model performed better. Lin and colleagues [17] proposed a model for classifying lung nodules that use a convolutional neural network with Taguchi architecture. The most important benefit of the Taguchi approach is the valuable information that can be discovered with fewer tests. Compared to other methods, the experimental findings showed that the Taguchi-based model employed by AlexNet reduced the training time. Al-Yasriy et al. [18] presented a computer-aided method for lung cancer diagnosis and classification that uses an AlexNet-based convolutional neural network architecture. The CT scan dataset for lung cancer was gathered from Iraqi hospitals and utilized for system testing and training. The system's results include a 96.403% F1 score, 95% specificity, 95.714% sensitivity, 97.102% precision, and 93.548% accuracy. The impact of Groups of Visual Geometry 19 (VGG19) on the 2014 ImageNet Challenge and 16 (VGG16) was examined by Patil et al. [19]. There were 16 weight layers in VGG16 and 19 weight layers in VGG19. The convolutional filter size of  $3 \times 3$  was employed in both networks, resulting in enhancements in the image recognition process, whereas  $224 \times 224$  RGB images made up the input size. The experimental findings demonstrated how depth representation improved state-of-the-art accuracy and helped categorize difficulties. Compared to alternative methods, both networks demonstrated great accuracy when evaluated on additional datasets. In a different study [20], a deep learning genetic algorithm was utilized to provide a method for early lung cancer detection. Three strategies were utilized in the preprocessing method: the picture was cropped into  $227 \times 227$  for VGG19 and  $224 \times 224$  for VGG16 for the AlexNet architecture; The contrast of the original image was enhanced by applying the histogram stretching technique; and the Noise was removed using a Wiener filter. Three CNN designs were utilized to handle images obtained from low-dose computed tomography (LDCT): AlexNet, VGG19, and VGG16. The most pertinent traits were chosen using a genetic algorithm. In the end, the classification of pulmonary lung nodules was studied using SVM classifiers, decision trees, and K-nearest neighbor. A dilated convolution network-based accurate lung segmentation technique and Geng et al. [21] reported VGG-16. The size of the corresponding field was shown to expand using dilated convolution, which employed a dilation rate parameter. Multi-scale convolution features were fused using the hyper-column features methodology to improve the robustness of the lung segmentation method. The ReLU (rectified linear unit) activation function and multilayer perceptron (MLP) were employed after the updated VGG16. A dice similarity coefficient of 0.9867 was attained by the procedure. Table 2 presents a comprehensive collection of lung cancer imaging datasets comprising various image types, including CT scans, X-rays, and histopathology images. For the purpose of creating and validating computer-aided diagnosis methods for lung cancer, these databases provide researchers and physicians with useful resources. A boosting strategy for VGG16 was presented in a different study [22] based on VGG16 to determine the pathogenic varieties of lung cancer. VGG16-T was made up of a  $3 \times 3$  kernel size of five layers. The boosting technique was discovered to improve efficiency and build a powerful classifier using just three weak classifiers. In the end, CT scans were utilized to identify the pathogenic type of lung cancer and the SoftMax function. Compared to the other methods, DenseNet, AlexNet, ResNet-34, and the VGG16-T testing results with boosting yielded an accuracy of 85%. Table 3 includes an overview of earlier relevant work. It is claimed that deep knowledge [7–10] is needed to get handmade characteristics, which is one of the limits of earlier studies.

The research [23–26] used unbalanced datasets and smaller picture sizes. Research works [12,13,15,27] concentrated on hybrid strategies that increased model complexity, whereas research works [28–30] employed various architectures to increase accuracy. A novel deep learning technique was proposed in [31] by altering the DenseNet201 model and incorporating additional layers into the original DenseNet framework to detect lung cancer. Maurya et al. [32] compared twelve machine learning algorithms using clinical data and found K-Nearest Neighbor and Bernoulli Naive Bayes as the most effective for early prediction. The results are based on classification and heat map correlation analysis. Hossain et al. [33] compared Machine Learning

(ML) models for lung cancer prediction, finding tree-based models balance accuracy and interpretability best, while neural networks excel but lack transparency. Key predictors include age, smoking history, and symptoms. The study called for larger datasets and improved interpretability for clinical use. Javed et al. [34] reviewed deep learning techniques, especially CNNs, for lung cancer detection and classification using medical imaging. They analyzed research from 2015–2024. The findings emphasized that deep convolutional neural networks play a vital role in improving diagnosis and reducing the burden on medical practitioners. Deep learning techniques, mainly CNNs, for lung cancer detection using medical imaging were discussed in [35]. The authors analyzed key datasets, compared studies, and explored explainable AI for real-world use.

**Table 2:** A summary of the dataset used for lung cancer detection

Ref.	Year	Method	Dataset
[36]	2020	InceptionV3, ResNet-50, VGG19	Chest X-ray +T
[37]	2020	ResNet-50	Chest CT
[38]	2020	CNN	Chest CT
[39]	2019	ResNet	Chest CT
[40]	2020	ResNet-50	Chest CT
[41]	2020	CNN	Chest CT
[42]	2020	AlexNet	Chest X-ray
[43]	2020	CNN + VGG16	X-ray Chest
[44]	2020	Resnet18, CNN, AlexNet and GAN	X-ray Chest
[45]	2020	DenseNet169, ResNet50, ResNet34	Chest X-ray
[46]	2020	ResNet-50 (COVID-ResNet)	X-ray Chest
[47]	2024	VGG19	Chest CT and PET-CT
[48]	2019	InceptionV3	LC25000
[49]	2021	VGG-16	CT images
[50]	2021	InceptionV3	LC25000
[51]	2022	InceptionV3	X-rays, CT and PET-CT
[52]	2022	ResNet 101	LC25000
[53]	2022	InceptionV3	LC25000

**Table 3:** Architecture of pre-trained models for lung classification

Disease	Name	Image type	Number of images
Lung cancer	RIDER Collections	CT	Approximately 280,000
Lung cancer	NSCLC-Radiomics-Genomics	CT	89
Lung cancer	NSCLC-Radiomics	CT	422
Lung cancer	NLST	CT	Approximately 200,000
Lung cancer	NIH-14 dataset	CT	14 lung diseases
14 lung diseases	NCI Genomic Data Commons	X-ray	112,120
Lung cancer	NCI Genomic Data Commons	Histopathology images	More than 575,000

(Continued)

**Table 3 (continued)**

Disease	Name	Image type	Number of images
Characterization of lung nodules: location and size	LUNA16	CT scans	888
Lung cancer	LIDC-IDRI	CT	1018
Lung cancer	Bowl 2017 dataset (Kaggle data science)	CT scans	601
Normal and nodules	JSRT dataset	CT and X-ray	93 and 154 nodules

This study presents a novel Computer Aided Diagnostic (CAD) System aimed at accurately classifying histopathological images for lung tissues to assist in the early diagnosis of lung cancer. Therefore, a robust detection system is necessary to identify lung cancer in its early stages. Hence, this study proposes a robust detection system using advanced deep learning algorithms and optimizers. The methodology encompasses dataset preparation, multi-scale feature processing, feature fusion, and hyperparameter tuning. Specifically, this study employs state-of-the-art algorithms, including AlexNet, VGG16, ResNet-50, VGG19, and the proposed model (CNN + VGG19). These models are used in conjunction with RMSprop, SGD, and Adam optimizers to enhance accuracy. Fig. 2 illustrates the process of using these algorithms and optimizers for lung cancer classification.

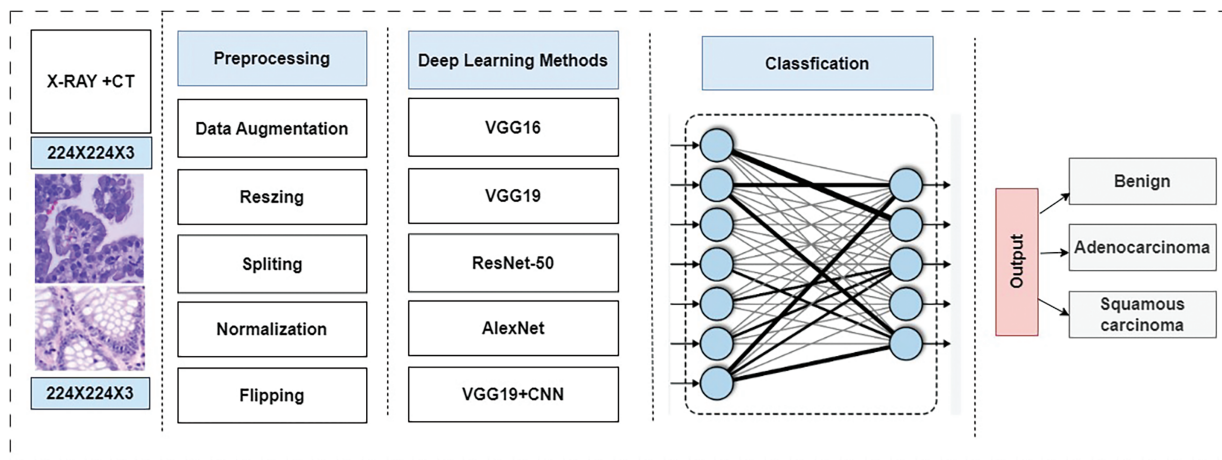


**Figure 2:** Block diagram for multiclassification based on pre-trained models

AlexNet to classify lung nodules. The hybrid design made use of both the LeNet layers and the AlexNet parameters. The LIDC-IDRI dataset provided 1018 CT images in total, which were used for the training and evaluation of the agile convolutional neural network. Achieving great accuracy required careful consideration of several factors, including learning rate, batch size, weight initialization, and kernel size. The framework obtained 0.822 accuracy and 0.877 AUC using  $7 \times 7$  kernel size, 32 batch size, and 0.005 learning rate. In this work, Dropout and Gaussian were also used. In 2012, Sharma et al. released AlexNet [14]. AlexNet won the 2012 ILSVRC, surpassing competitors with a top 5 error rate of 15.3%, demonstrating a widespread advancement in CNN performance. The researchers in [15] proposed two designs for the categorization of pulmonary nodules: hybrid 3D-CNN and straight 3D-CNN. Although the classifiers in the

two models were different, the feature extraction technique remained the same. The pulmonary CT images were classified Using the 3D-CNN model's SoftMax classifier, while the hybrid 3D-CNN employed an SVM classifier based on the radial basis function (RBF). The results of the experiment showed that the accuracy of straight 3D-CNN models and the hybrid 3D-CNN was higher. However, in comparison to a SoftMax classifier for the 3D-CNN model, the strategy achieved 91.9% precision, 88.53% sensitivity, 94.23% specificity, and 91.8% accuracy.

Ali et al. [16] made use of convolutional neural networks to classify lung tumors. A final fully linked layer, a dropout layer, and a pooling layer, and two convolution layers made up the proposed CanNet architecture. The accuracy achieved by artificial neural networks was 72.50%, while LeNet achieved an accuracy of 56.0%, and CanNet achieved an accuracy of 76.00%. In comparison to the LeNet and ANN networks, the CanNet model performed better. Lin and colleagues [17] proposed a model for classifying lung nodules that use a convolutional neural network with Taguchi architecture. The most important benefit of the Taguchi approach is the valuable information that can be discovered with fewer tests. Compared to other methods, the experimental findings showed that the Taguchi-based model employed by AlexNet reduced the training time. Al-Yasriy et al. [18] presented a computer-aided method for lung cancer diagnosis and classification that uses an AlexNet-based convolutional neural network architecture. The CT scan dataset for lung cancer was gathered from Iraqi hospitals and utilized for system testing and training. The system's results include a 96.403% F1 score, 95% specificity, 95.714% sensitivity, 97.102% precision, and 93.548% accuracy. The impact of Groups of Visual Geometry 19 (VGG19) on the 2014 ImageNet Challenge and 16 (VGG16) was examined by Patil et al. [19]. There were 16 weight layers in VGG16 and 19 weight layers in VGG19. The convolutional filter size of  $3 \times 3$  was employed in both networks, resulting in enhancements in the image recognition process, whereas  $224 \times 224$  RGB images made up the input size. The experimental findings demonstrated how depth representation improved state-of-the-art accuracy and helped categorize difficulties. Compared to alternative methods, both networks demonstrated great accuracy when evaluated on additional datasets. Elnakib et al. [20] employed a deep learning genetic algorithm to provide a method for early lung cancer detection. Three strategies were utilized in the preprocessing method: the picture was cropped into  $227 \times 227$  for VGG19 and  $224 \times 224$  for VGG16 for the AlexNet architecture; The contrast of the original image was enhanced by applying the histogram stretching technique; and the Noise was removed using a Wiener filter. Three CNN designs were utilized to handle images obtained from low-dose computed tomography (LDCT): AlexNet, VGG19, and VGG16. The most pertinent traits were chosen using a genetic algorithm. In the end, the classification of pulmonary lung nodules was studied using K-nearest neighbor SVM classifiers, decision trees, and (KNN). A dilated convolution network-based accurate lung segmentation technique and VGG-16 were reported by Geng et al. [21]. The size of the corresponding field was shown to expand using dilated convolution, which employed a dilation rate parameter. Multi-scale convolution features were fused using the hyper-column features methodology to improve the robustness of the lung segmentation method. The ReLU activation function and multilayer perceptron (MLP) were employed after the updated VGG16. A dice similarity coefficient of 0.9867 was attained by the procedure. Table 3 presents a comprehensive collection of lung cancer imaging datasets comprising various image types, including CT scans, X-rays, and histopathology images. For the purpose of creating and validating computer-aided diagnosis methods for lung cancer, these databases provide researchers and physicians with useful resources. A boosting strategy for VGG16 was presented in a different study [22] based on VGG16 to determine the pathogenic varieties of lung cancer. VGG16-T was made up of a  $3 \times 3$  kernel size of five layers. The boosting technique was discovered to improve efficiency and build a powerful classifier using just three weak classifiers. In the end, CT scans were utilized to identify the pathogenic type of lung cancer and the SoftMax function. Compared to the other methods, DenseNet, AlexNet, ResNet-34, and the VGG16-T testing results with boosting yielded an accuracy



of 85%. Table 3 includes an overview of earlier relevant work. It is claimed that deep knowledge [7–10] is needed to get handmade characteristics, which is one of the limits of earlier studies.

The research [23–25] used unbalanced datasets and smaller picture sizes. Research works [12,13,15] concentrated on hybrid strategies that increased model complexity, whereas research works [28–30] employed various architectures to increase accuracy. Classifying histopathological images for lung tissues to assist the early diagnosis of lung cancer. Therefore, a robust detection system is necessary to identify lung cancer in its early stages. This study proposes a robust detection system using advanced deep learning algorithms and optimizers. The methodology encompasses dataset preparation, multi-scale feature processing, feature fusion, and hyperparameter tuning. Specifically, this study employs state-of-the-art algorithms, including AlexNet, VGG16, ResNet-50, VGG19, and the proposed model (CNN + VGG19). These models are used in conjunction with RMSprop, SGD, and Adam optimizers to enhance accuracy. Fig. 2 illustrates the process of using these algorithms and optimizers for lung cancer classification.

### 3 Proposed Methodology

This study proposes a novel Computer Aided Diagnostic (CAD) System to accurately classify histopathological images for lung tissues to assist in early lung cancer detection. Therefore, a robust detection system is necessary to diagnose lung cancer in its early stages. This approach efficiently compares various models' performance in lung and colon cancer image classification tasks. Fig. 3 illustrates the methodology employed in the research, which combines a conventional neural network (CNN) with a pre-trained VGG19 model. In addition, for the training and testing model, this study uses the LC25000 dataset, allocating 75% for training, 12.5% for testing, and 12.5% for validation. It also implements 5-fold cross-validation, where the dataset is divided into five-fold, and one-fold is used for testing to ensure robustness and generalizability. In contrast, the remaining folds are used for training and validation. In addition, the proposed method allows to evaluate the performance of various models, including AlexNet, VGG16, and ResNet-50.

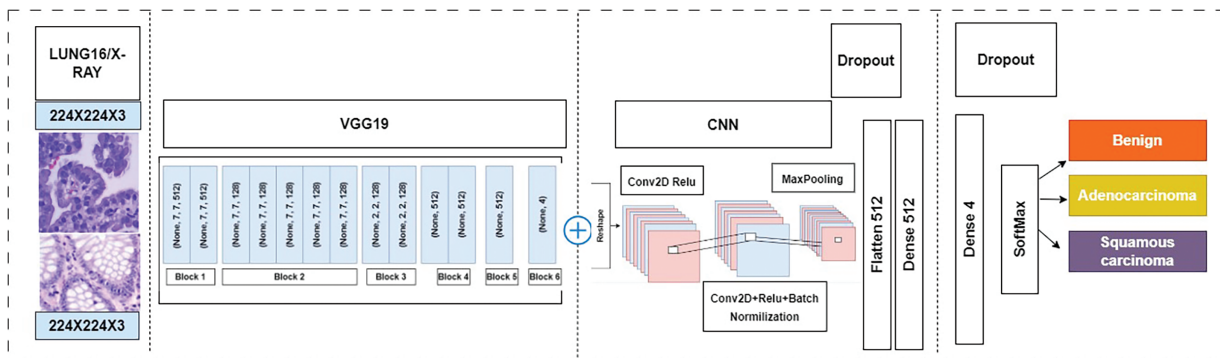


Figure 3: Proposed model combined CNN + VGG19 for lung cancer detection

Fig. 2 illustrates the process of using these algorithms and optimizers for lung cancer classification [54].

This approach efficiently compares various models' performance in lung and colon cancer image classification tasks. Fig. 3 [54] illustrates the methodology employed in the research, which combines a conventional neural network (CNN) with a pre-trained VGG19 model that was initially proposed in [54]. In addition, for the training and testing model, this study utilizes the LC25000 dataset, allocating 75% for training, 12.5% for testing, and 12.5% for validation. It also implements five-fold cross-validation, where the dataset is divided into five-fold, and one-fold is utilized for testing to ensure robustness and generalizability.

In contrast, the remaining folds were used for training and validation. In addition, the proposed method allows to evaluate the performance of various models, including AlexNet, VGG16, and ResNet-50.

### A. Dataset Preparation

The datasets that are used are first augmented, and the dataset is a comprehensive collection of 25,000 images with five distinct classes. Each class contains 5000 images to ensure that there is a balance between the classes and that more photographs are utilized than necessary. The images are high quality with a pixel size of  $768 \times 768$  and are stored in jpeg format for efficient compression and transfer. The dataset was converted into a single zip file with a total size of 1.85 GB to facilitate easy access and download. Once downloaded and extracted, the dataset is organized into a clear and intuitive folder structure. The main folder `lung_colon_image_set` contains two primary subfolders: `colon_image_sets` and `lung_image_sets`. These subfolders are further divided into secondary subfolders, each containing specific types of images. Within the `colon_image_sets` folder, there are two subfolders: ‘`colon_aca`’, housing 5000 images of colon adenocarcinomas, and `colon_n`, containing 5000 images of benign colonic tissues. In the `lung_image_sets` there are three folders: (`lung_aca`, 5000 images of adenocarcinomas), ‘`lung_aca`’, featuring 5000 images of lung squamous cell carcinomas, and ‘`lung_n`’, with 5000 images of benign lung tissues [48]. Fig. 1 shows the category of lung and colon histopathology cancer diseases, and Fig. 4 depicts the random samples from the LC25000 dataset.

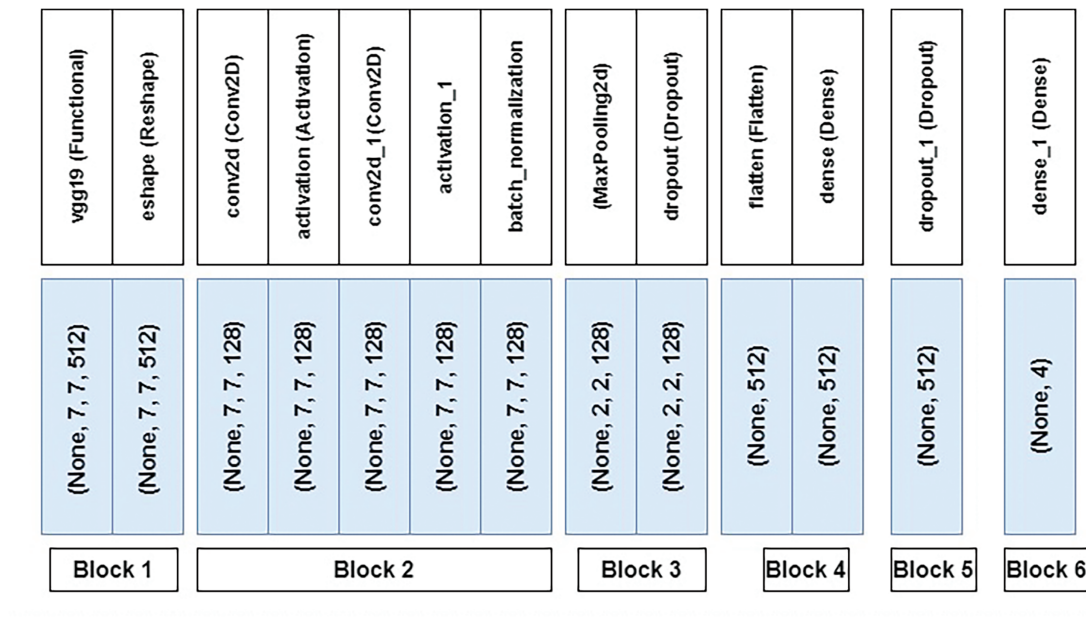


Figure 4: Number of layers and blocks in combined approach (CNN + VGG19)

### B. Feature Fusion

All the Preprocessing Techniques are used with the help of an image data generator. The processing techniques used in the Image Data Generator are applied only to the training dataset.

#### i. Pixel Normalization

The normalization process involves a simple element-wise division of the pixel values by 255, the maximum possible value, applied uniformly across all color channels, regardless of the image’s original dynamic range [9].

### ***ii. Pixel Centering***

The image data processing pipeline involves a sequence application of normalization and centering transformations. Normalization rescales the pixel values to a standardized range, typically between 0 and 1, to mitigate feature dominance and facilitate model convergence. Subsequent centering involves subtracting the mean value from the normalized pixel values that remain within the desired range, maintaining the image's visual integrity and preventing erroneous reading. Centering requires calculating the mean pixel value before subtracting it from the pixel values. The mean can be computed using various methods, including:

- Per Image Mean
- Per Mini Batch Mean (under SGD)
- Per Training Dataset Mean

In addition, the mean pixel value per image is calculated. For color images, centering can be applied either globally or locally:

Global centering: subtracting the mean pixel value computed across all color channels.

Local centering: subtracting the mean pixel value computed separately for each color channel

### ***iii. Pixel Standardization***

The distribution of pixel values often exhibits a normal or Gaussian profile characterized by a bell-shaped curve. The distribution can manifest at various levels, contains per image, per min batch, across the entire training, globally color channels, and locally per color channel. Transferring the pixel value distribution into a standard Gaussian distribution can be beneficial, involving both centering and scaling operations. This process is known as standardization. Standardization is often preferred over normalization and centering alone, as it yields zero-centered values with small input values, typically ranging from  $-3$  to  $3$ , depending on the dataset specifics [9].

## **C. Combined CNN + VGG19**

This study combines CNN + VGG19 model lung and colon cancer diagnosis from histological images utilizing a VGG19 pre-trained model augmented with additional layers for enhanced feature extraction and classification. The architecture of the proposed model is illustrated in Fig. 5, with details of the layers and blocks used. The proposed model takes input image size  $768 \times 768$  pixels, derived from lung and colon histological datasets. Initially, the VGG19 model performs preliminary feature extraction. This is followed by two custom CNN blocks designed for further feature refinement. Each CNN block contains Convolutional layers with ReLU activation, Batch normalization, Max pooling, and dropout layers to prevent overfitting. Following these CNN blocks, a flattened layer transforms the multi-dimensional output into a one-dimensional vector, which is then fed into a dense layer containing 512 neurons. The dense layer, equipped with a dropout mechanism, serves as the primary classifier, and the final dense layer, with neurons corresponding to the number of classes, uses a SoftMax activation function to classify the images for three classes.

## **D. Hyperparameter Tuning**

CNN comprises numerous hyperparameters and parameters such as weights, neurons, layers, stride, filter size and biases, learning rate, and optimization functions. Convolution layers are important for extracting deep features from the images [46]. Two types of filters: small filters used for filters focused on fine-grained details and large filters used for coarse-grained features.

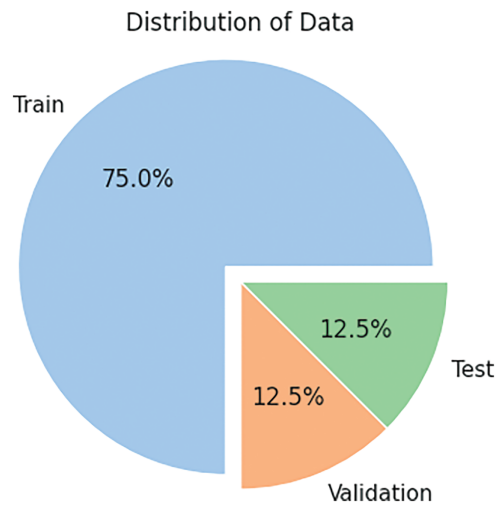


**Figure 5:** Distribution of dataset

The pioneering LeNet model, introduced by LeCun et al. in 1988, employed a  $5 \times 5$  convolutional filter with a stride of 2 for zip code recognition, followed by a  $2 \times 2$  pooling layer with a stride of 2; this groundbreaking work laid the foundation for future advancements. A seminal moment in deep learning occurred in 2012 when AlexNet, a convolutional neural network (CNN) architecture, triumphed in the ImageNet Large-scale visual recognition challenge (ILSVRC). This achievement marked a paradigm shift in computer vision, as AlexNet's innovative design comprised five convolution layers. Three pooling layers and fully connected (FC) layers introduce the rectified linear unit (ReLU) activation function to CNNs. The visual Geometry Group (VGG) network, another influential architecture, is available in two variants: VGG18, consisting of 16 layers, and VGG19, comprising 19 layers. As the number of layers increases, the filter size decreases, demonstrating a tradeoff between depth and granularity. This research uses a suite of esteemed CNN architectures, including AlexNet, VGG16, ResNet-50, and VGG19, to classify lung cancer using the LC25000 dataset.

This research uses a suite of esteemed CNN architectures, including AlexNet, VGG16, ResNet-50, and VGG19, to classify lung cancer using the LC25000 dataset. The basic configuration of these pre-trained models is summarized in Table 4. The pros and cons of CNN-based pre-trained methods are discussed in Table 5, highlighting their advantages in training, improved performance, and high accuracy while also noting their limitations, including high memory requirements, slow training, and impractical training times for real-world applications.

**Table 4:** The architecture of pre-trained models for lung classification

VGG16	VGG19	AlexNet	ResNet-50	CNN + VGG19
(Conv-Layer 1-1)	(Conv-Layer 1-1)	( $11 \times 11$ Conv-96)	( $7 \times 7$ Conv-64)	(Functional, 7, 7, 512)
(Conv-Layer 1-2)	(Conv-Layer 1-2)	( $3 \times 3$ Maxpool, stride 2)	( $7 \times 7$ Conv-64)	(Reshape, 7, 7, 512)
<b>Pooling layer</b>	<b>Max pooling layer</b>	( $5 \times 5$ Conv-256)	<b>X3, Stage 1</b>	(Conv2D, 7, 7, 512)

(Continued)

**Table 4 (continued)**

VGG16	VGG19	AlexNet	ResNet-50	CNN + VGG19
(Conv-Layer 2-1)	(Conv-Layer 2-1)	(3 × 3 Maxpool, stride 2)	(1 × 1 Conv-64)	(Activation, 7, 7, 512)
(Conv-Layer 2-2) <b>Pooling layer</b>	(Conv-Layer 2-2) <b>Max pooling layer</b>	(3 × 3 Conv-384) (3 × 3 Conv-384)	(3 × 3 Conv-64) (1 × 1 Conv-256)	(Conv2D, 7, 7, 512) (activation_1, 7, 7, 512)
(Conv-Layer 3-1)	(Conv-Layer 3-1)	(3 × 3 Conv-384)	<b>X3, Stage 2</b>	(BatchNormalization, 7, 7, 512)
(Conv-Layer 3-2)	(Conv-Layer 3-2)	Dense (4096)	(1 × 1 Conv-128)	(MaxPooling2d, 7, 7, 512)
(Conv-Layer 3-3) <b>Pooling layer</b>	(Conv-Layer 3-3) (Conv-Layer 3-4)	Dense (4096) Dense (1000)	(3 × 3 Conv-128) (1 × 1 Conv-512)	(Dropout, 7, 7, 512) (Flatten, 7, 7, 512)
(Conv-Layer 4-1)	<b>Max pooling layer</b>		<b>X3, Stage 3</b>	(Dense, 7, 7, 512)
(Conv-Layer 4-2)	(Conv-Layer 4-1)		(1 × 1 Conv-256)	(Dropout, 7, 7, 512)
(Conv-Layer 4-3) <b>Pooling layer</b>	(Conv-Layer 4-2) (Conv-Layer 4-3)		(3 × 3 Conv-256) (1 × 1 Conv-1024)	(Dense, 7, 7, 512)
(Conv-Layer 4-1)	(Conv-Layer 4-4)		<b>X3, Stage 4</b>	
(Conv-Layer 4-2)	<b>Max pooling layer</b>		(1 × 1 Conv-512)	
(Conv-Layer 4-3) <b>Pooling layer</b>	(Conv-Layer 4-1) (Conv-Layer 4-2)		(3 × 3 Conv-512) (1 × 1 Conv-256)	
<b>Dense layer</b>	(Conv-Layer 4-3)		Average pooling	
<b>Dense layer</b>	(Conv-Layer 4-4)		Dropout	
<b>Dense layer</b>	<b>FC1</b>		Relu	
	<b>FC2</b>		Dropout	
			SoftMax	

**Table 5:** Benefits and limitations of CNN-based pre-trained methods

Model	Pros	Cons
AlexNet	<ul style="list-style-type: none"> <li>• Uses ReLU activation for faster training</li> <li>• Employs dropouts to prevent overfitting</li> <li>• Uses the data augmentation techniques to improve the performance of model robustness.</li> </ul>	<ul style="list-style-type: none"> <li>• Consumes substantial memory, making it less efficient for deployment on resource constrained devices.</li> <li>• Require extra computation efforts</li> </ul>
VGG16	<ul style="list-style-type: none"> <li>• The model is ideal for benchmarking and specific tasks.</li> </ul>	<ul style="list-style-type: none"> <li>• The training model is lazy/slow</li> </ul>
VGG19	<ul style="list-style-type: none"> <li>• More perfect and efficient VGG19</li> </ul>	<ul style="list-style-type: none"> <li>• Requires high memory</li> </ul>

(Continued)

**Table 5 (continued)**

Model	Pros	Cons
ResNet-50	<ul style="list-style-type: none"> <li>A network can be built using hundreds or even thousands of residual layers, which can be trained to achieve high accuracy.</li> <li>This approach also addresses the gradient problem using identify mapping to enable more effective training</li> </ul>	<ul style="list-style-type: none"> <li>Training from scratch requires a significant amount of time, typically spanning several weeks, making it impractical and unrealistic for real-world applications where efficiency and timely results are crucial.</li> </ul>

#### 4 Results and Discussion

This study uses the LC25000 dataset to comprehensively evaluate the performance of the proposed model (CNN + VGG19) as shown in Algorithm 1, against the other fine-tuned or pre-trained models for lung cancer detection. Specifically, it trains the model on a three-class classification problem encompassing Adenocarcinoma, Squamous Cell Carcinoma, and Benign. The experimental design allocates 75% of the dataset for training and rigorously evaluates the model performance on the test set 12.5% using the metrics listed in Table 6. In addition, this research investigates implemented 5-fold cross-validation to ensure robustness and generalizability. Table 6 indicates all pre-trained models performed exceptionally well on the LC25000 dataset, achieving accuracy rates exceeding 90%. The proposed model achieved the highest accuracy, 99.04%. Surpassing the performance of individual pre-trained models. These findings demonstrate the effectiveness of using pre-trained models and combining CNN architectures for lung cancer detection.

---

#### Algorithm 1: Proposed (CNN + VGG19) Ensemble for Cancer Detection

---

*Input: Image dataset, Labels*

*Output: Classification Metrics*

*Load image dataset and labels.*

*Preprocess images (resizing, normalization).*

*Split dataset into training and testing sets.*

*Initialize VGG19 model (pretrained weights, remove top layers).*

*Initialize custom CNN architecture*

*Extract features from images using VGG19 and CNN.*

*Concatenate features from VGG19 and CNN.*

*Train Random Forest, SVM, and Logistic Regression on concatenated features.*

*Make predictions on test set using trained classifiers.*

*Combine predictions using majority voting or average probability.*

*Evaluate ensemble classifier using metrics (accuracy, precision, recall, F1-score).*

*Plot Accuracy and loss with Confusion matrix.*

---

**Table 6:** Metrics used for lung cancer detection

Task	Metric	Equation	Description
Classification	Accuracy	$Accuracy = \frac{TP + TN}{TP + TN + FP + FN}$	Evaluate the effectiveness of models in terms of positive and negative instances
Classification	Sensitivity	$Sens = \frac{TP}{TN + TP}$	Compute the true positive rate (sensitivity), which measures the model's accuracy in identifying actual positive cases.
Classification	Specificity	$Spec = \frac{TN}{TN + FP}$	Determine the percentage of real negative situations that are correctly classified as negative and true negative rate
Classification	Precision	$Prec = \frac{TP}{TP + FP}$	The precision can be calculated as the percentage of real positive identification among positive identification that are accurately identified
Classification and segmentation	F1 score	$F1 = 2X \frac{Precision + Recall}{Precision + Recall}$	Harmonic average of precision and recall
Classification	ROC	$ROC = \frac{\sqrt{SNS^2 - SPC^2}}{\sqrt{2}}$	Graphical representation of sensitivity

This study comprehensively compares state-of-the-art CNN architectures—AlexNet, VGG16, VGG19, and ResNet-50 for lung cancer detection, utilizing various optimizers (SGD, Adam, and RMSprop). The performance of each architecture is thoroughly evaluated and validated in terms of accuracy, employing binary cross-entropy loss. The respective detection algorithms achieve the results presented. The performance is examined with Python 3.8, the Keras tool, a batch size of 20, 50 epochs, and a learning rate of 0.001. Several optimizers are utilized to analyze each design's performance, and statistical metrics such as accuracy, specificity, sensitivity, and F1 score, as well as negative predictive value, false omission rate, and predictive value, are examined to determine how well each architecture detects lung cancer. This thorough examination facilitates the section on the best strategy for lung cancer diagnosis by illuminating the advantages and disadvantages of each design and optimizer combination.

This study assesses how well the indicated method classified nodules based on several well-recognized standards [15,27]. These metrics evaluate how well the model differentiates between benign lung tissue, lung squamous cell cancer, colon adenocarcinoma, lung adenocarcinoma, and benign lung tissue.

The capacity of the model to reliably detect malignant situations is observed in the image.

A key aspect of accurate sickness detection is the illustration's ability to show how effectively the model can consistently identify instances of illness. A crucial measure, accuracy, shows the total percentage of correctly classified data. This study evaluates its specificity, AUC, and F1 score to assess the proposed model classification performance on lung and colon; specificity measures the accurate identification of lung and

colon cancer, while AUC under the receiver operating characteristic (ROC) evaluates the model's ability to distinguish between lung and colon. The following assessment metrics can be calculated in [Table 6](#).

[Table 6](#) presents various metrics utilized to evaluate the performance of lung cancer detection models. These metrics provide insights into different aspects of the model's performance, enabling a comprehensive understanding of its strengths and weaknesses. The terms TP, TN, FN, and FP are employed in the subsequent calculations. Nodules that are correctly identified as benign and malignant are considered true positives. True negativity, or TN, is a metric that measures the number of benign nodules that are accurately recognized. The number of malignant nodules that were mistakenly diagnosed as benign is known as false negative, or FN. The term "false positive," or "FP," describes the quantity of benign nodules that were incorrectly classified as cancerous.

The novelty of this study lies in the integration of CNN and VGG19 for lung and colon cancer detection, combining deep feature extraction, high-performance filtering, and ensemble learning to enhance diagnostic accuracy. Unlike existing studies, it introduces a unique feature extraction technique using multiple transfer learning models for robust feature representation. In addition, a comprehensive evaluation of the LC25000 dataset across various metrics validates the effectiveness of the proposed approach.

[Figs. 6](#) and [7](#) depict a comprehensive evaluation of the proposed CNN + VGG19 model and its comparison to other pre-trained CNN-based models, namely AlexNet, VGG16, VGG19, and ResNet50, for the classification of lung and colon cancer. The performance metrics demonstrated in [Fig. 7](#) reveal that the proposed CNN + VGG19 approach surpassed other models, achieving an exceptional accuracy of 99.04%. VGG19 secured the second-highest accuracy of 99.02%, closely trailing the proposed model. This remarkable performance highlights the effectiveness of the CNN + VGG19 model in using the strengths of both architectures to improve cancer classification accuracy. The findings indicate that the proposed model's ability to learn and adapt to complex patterns in medical images can lead to enhanced diagnostic precision, making it a valuable tool for clinical applications. Future research directions can include exploring the model's generalizability across diverse cancer types and investigating the impact of transfer learning on its performance.

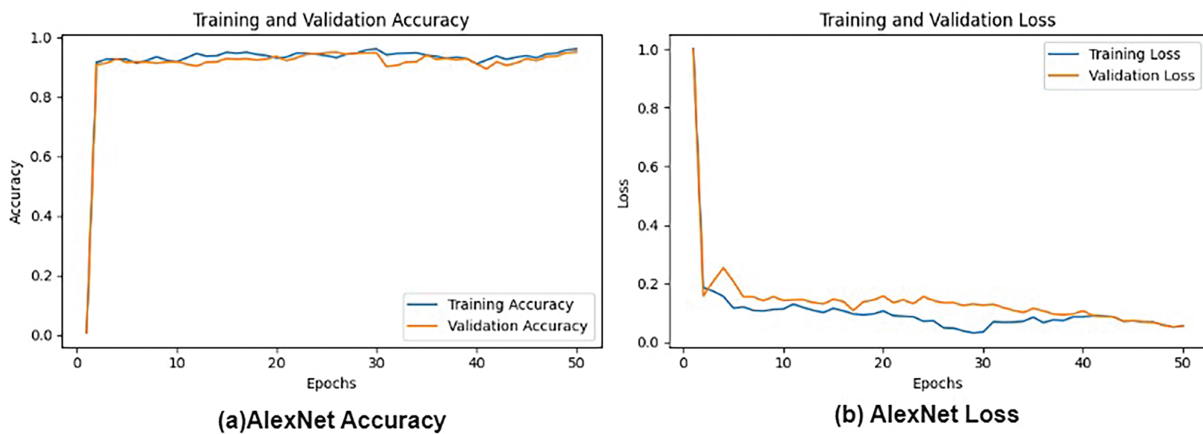


**Figure 6:** (Continued)



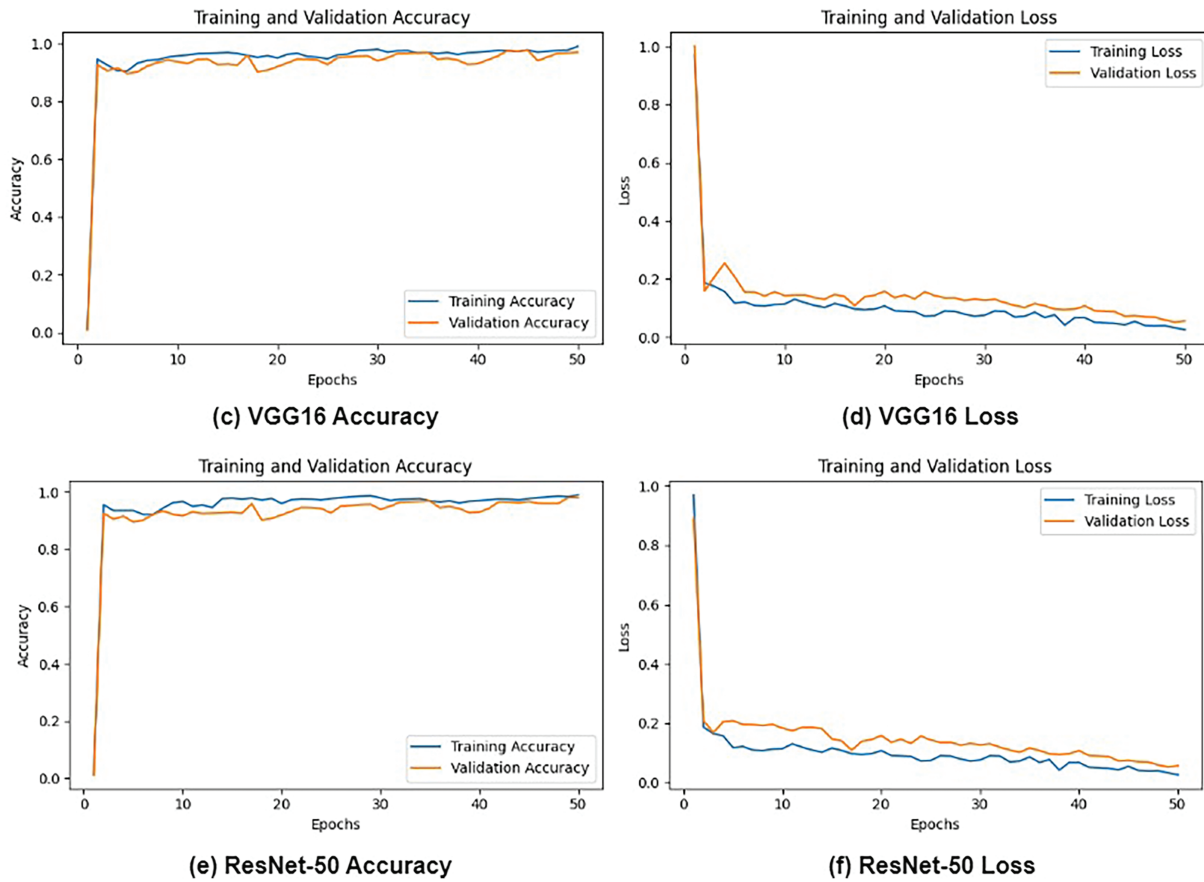


Figure 6: Loss and Accuracy: (a) AlexNet Accuracy, (b) AlexNet Loss and, (c) VGG16 Accuracy, (d) VGG16 Loss, (e) ResNet-50 Accuracy, and (f) ResNet-50 loss

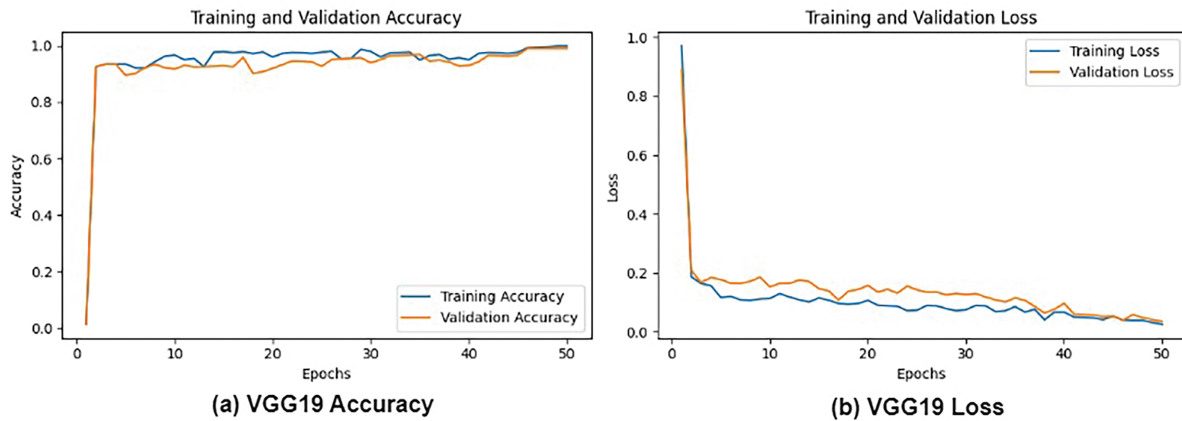
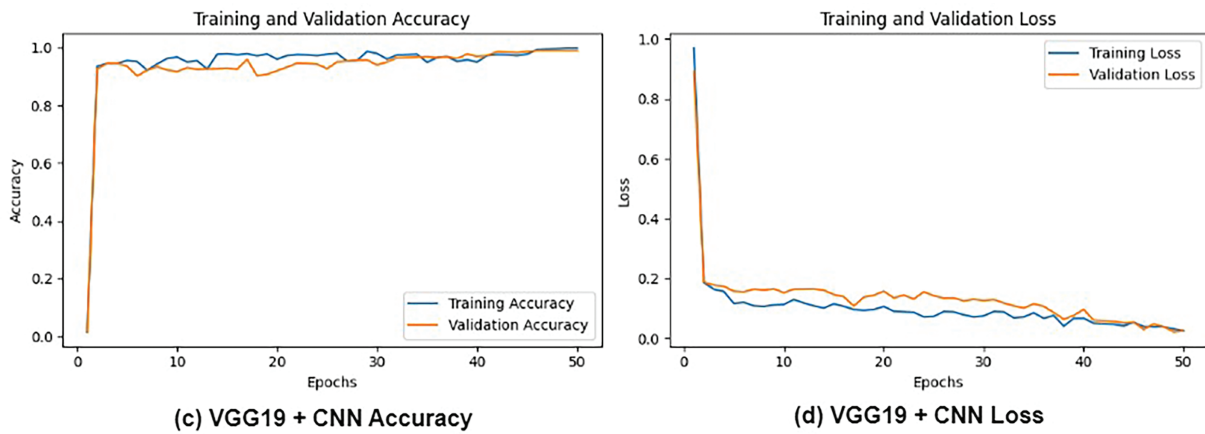
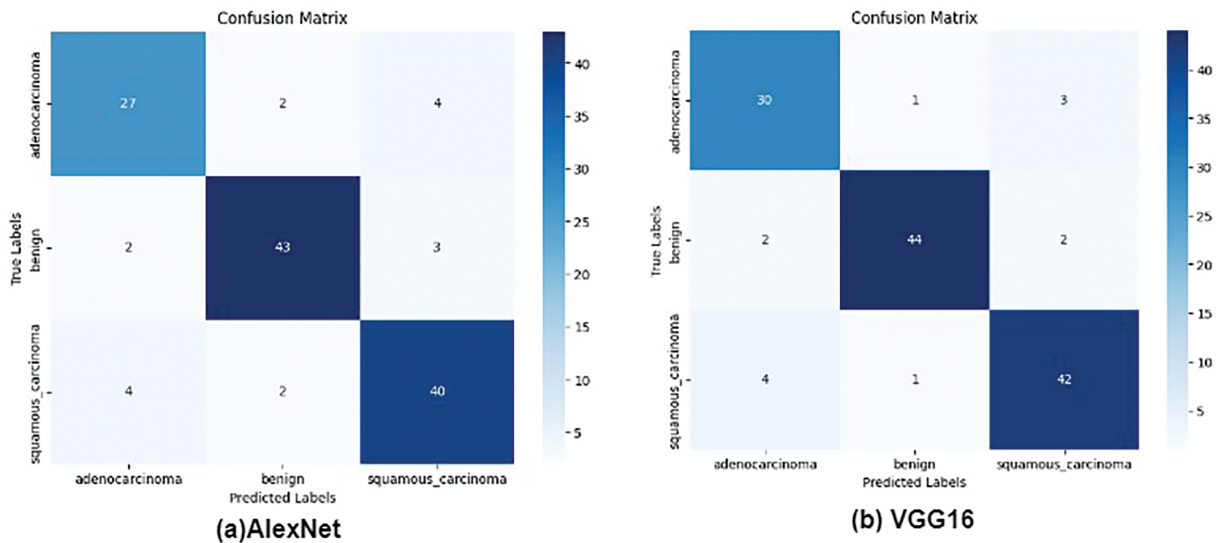


Figure 7: (Continued)

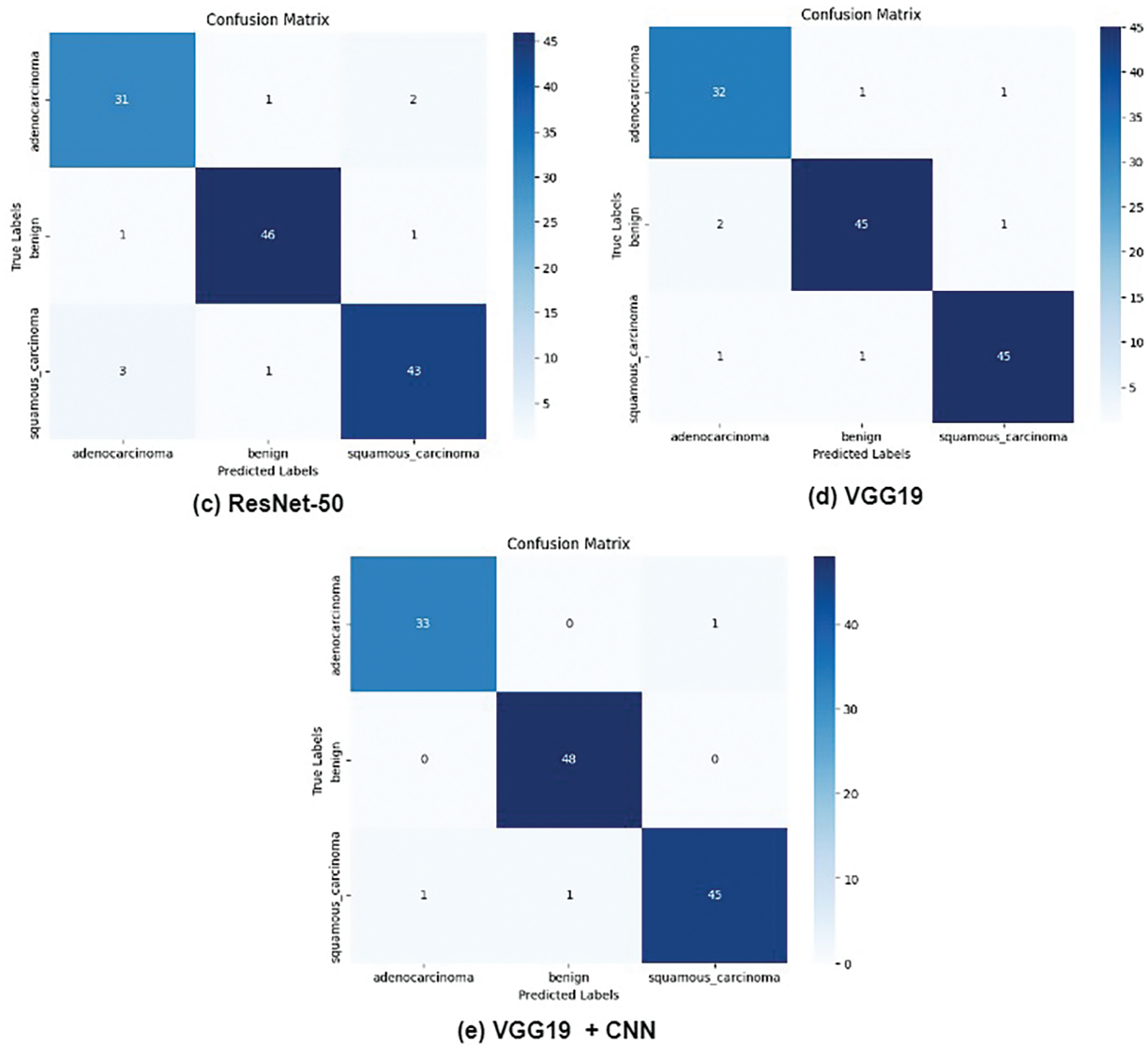


**Figure 7:** Loss and accuracy: (a) VGG19 Accuracy, (b) VGG19 Loss and, (c) CNN + VGG19 Accuracy, and (d) CNN+VGG19 Loss

Fig. 8 presents the confusion matrices for all evaluated models, providing a detailed comparison of the performance of AlexNet, VGG16, VGG19, ResNet50, and the proposed CNN+ VGG19 model in classifying three types of cancer diseases: Lung\_n (normal lung tissue), Lung\_aca (lung adenocarcinoma), and Lung\_scc (lung squamous cell carcinoma). The confusion matrices reveal that the proposed CNN + VGG19 model achieves outstanding results, demonstrating superior performance across all three cancer types. The proposed model exhibits exceptional accuracy in classifying Lung\_scc, with significantly higher true positive and lower false negative rates than the other models. The results also indicate that the proposed model distinguishes between normal lung tissue (Lung\_n) and cancerous images, achieving a high true negative rate and low false positive rate. This is critical for reducing the likelihood of misdiagnosis and ensuring accurate cancer detection. The results demonstrate exceptional diagnostic performance of the proposed model, with AUC values exceeding 0.99 for all three classes.

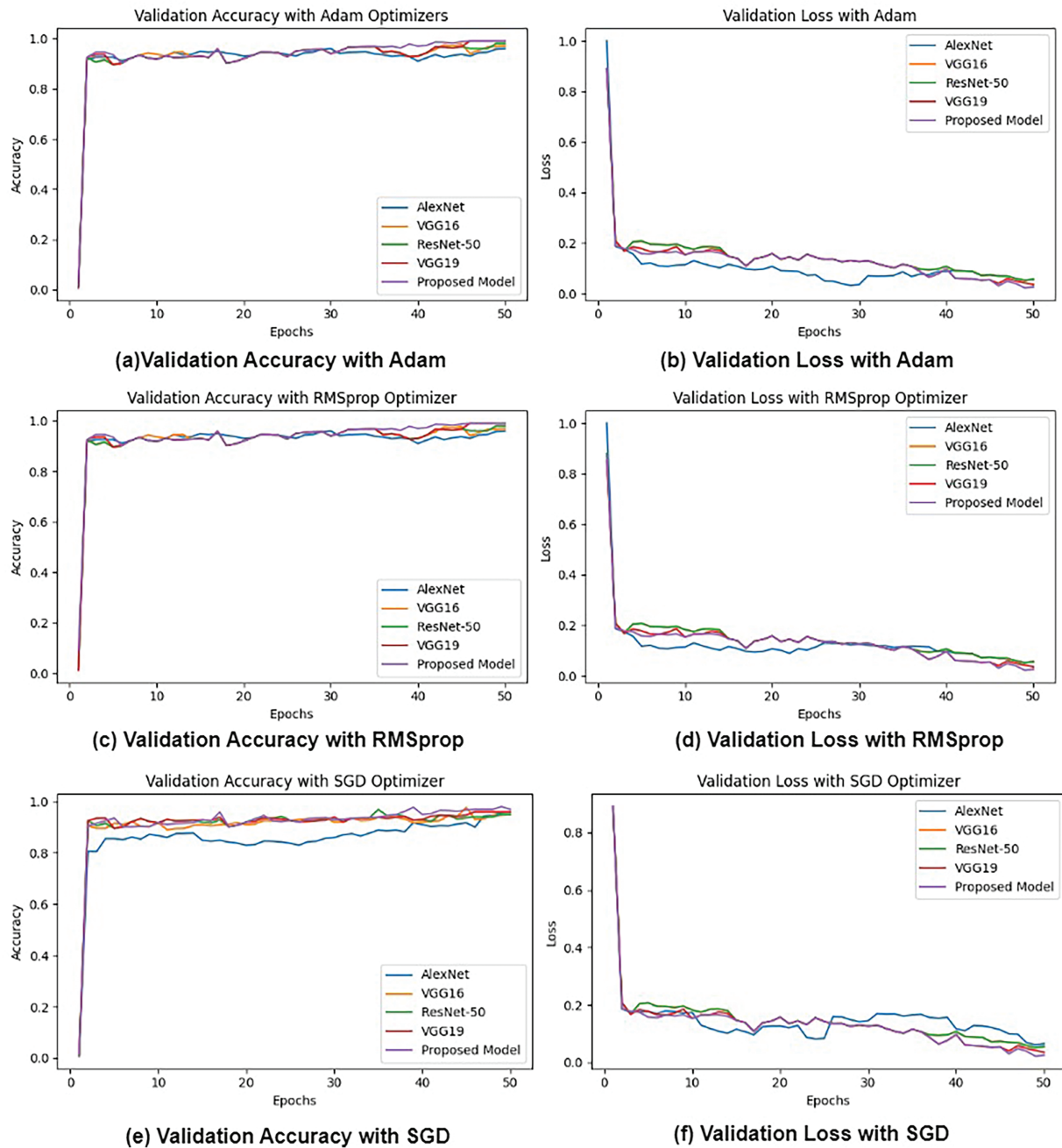


**Figure 8:** (Continued)



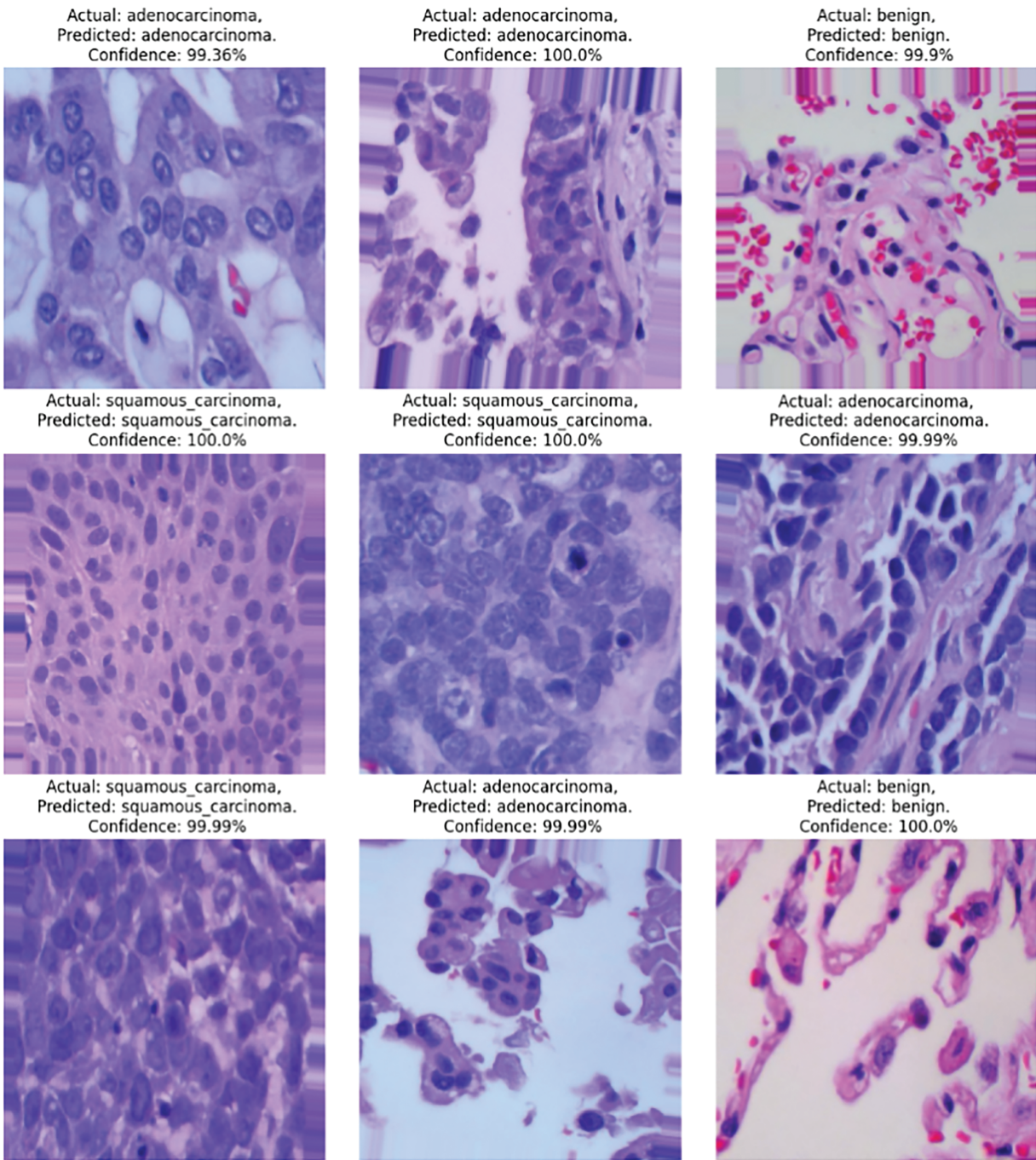
**Figure 8:** True and false prediction of pre-trained models for cancer classes

Fig. 9 presents the validation performance of various hyperparameters on pre-trained models (AlexNet, VGG16, VGG19, and ResNet-50) for lung cancer detection using different optimizers (SGD, Adam, and RMSprop). The proposed approach achieved outstanding results with Adam (99.04% accuracy) and RMSprop (99.03% accuracy), but SGD performance is slightly low.



**Figure 9:** Validation performance with optimizers (Adam, RMSprop, and SGD)

**Fig. 10** compares the actual cancer images and the predicted images generated by the proposed CNN+VGG19 model for lung cancer detection. The figure demonstrates the exceptional performance of the proposed model in accurately detecting and predicting lung cancer, particularly for lung adenocarcinoma (lung\_aca) and lung squamous cell carcinoma (lung\_scc).



**Figure 10:** Proposed model prediction on lung cancer detection

Fig. 11 illustrates the training and testing accuracy of various deep learning models, where the graph indicates a visual comparison of the performance of these models, highlighting the superiority of the proposed (VGG19 + CNN) model. The training accuracy curves demonstrate that the proposed model achieves rapid convergence and consistently high accuracy throughout the training process, indicating effective learning and adaptation to the dataset. In contrast, the other models exhibit slower convergence and lower training accuracy, indicating limitations in their ability to capture complex patterns in the data.

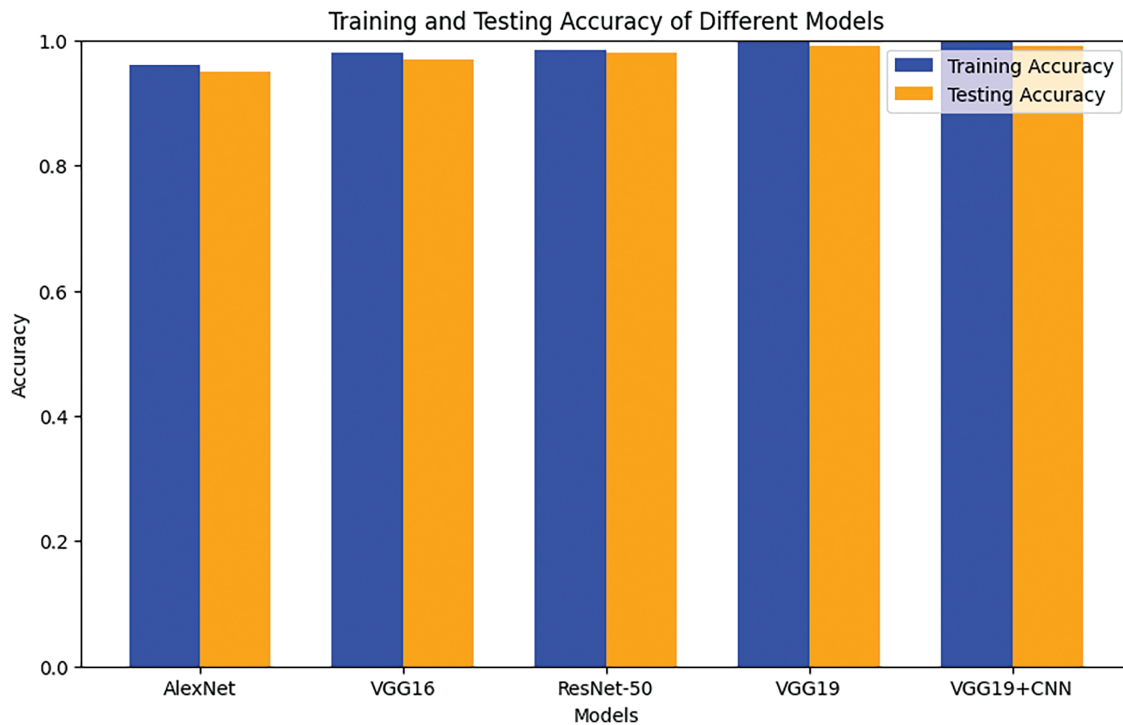


**Figure 11:** Training and testing of CNNs-based pretrained models

The study evaluates the proposed CNN + VGG19 model against pre-trained models (AlexNet, VGG16, VGG19, and ResNet50) for lung and colon cancer classification. Results show that CNN + VGG19 outperforms all models, achieving 99.04% accuracy, with VGG19 closely following at 99.02%. Confusion matrices highlight its superior classification of cancer types, reducing false positives and misdiagnoses. The model performs exceptionally well with Adam and RMSprop optimizers, as shown in the validation tests. ROC curves confirm strong class separation, while training accuracy graphs demonstrate rapid convergence and high performance, highlighting the model's effectiveness in medical diagnostics.

Table 7 shows that the proposed (CNN + VGG19) model achieves the highest performance across all classes, with F1-scores of 99% for Lung\_n and Lung\_scc, and 98% for Lung\_aca. ResNet50 and VGG19 also perform well, achieving F1 scores above 97% for all classes. In contrast, AlexNet and VGG16 have relatively lower performance, with F1 scores ranging from 94% to 96% across classes.

**Table 7:** The performance of pre-trained CNNs for lung cancer classification (Lung\_b (Benign), Lung\_aca (Lung adenocarcinoma), and Lung\_scc (Squamous Cell Carcinoma)). Values are in percentage

Class	AlexNet	VGG16	VGG19	ResNet50	Proposed model
	P R F1	P R F1	P R F1	P R F1	P R F1
Lung_b	95 94 94	97 98 97	97 96 98	95 94 94	99 99 99
Lung_aca	95 96 95	98 98 98	97 96 97	95 94 94	98 98 98
Lung_scc	94 96 95	98 98 96	97 97 97	98 97 97	99 99 99

**Table 8** lists an analysis of the proposed study compared to previous techniques. The table discusses how researchers have proposed various deep learning-based methods for cancer diagnosis using histopathological images, achieving high accuracy rates. For instance, Masud et al. and Hatuwal et al. reported accuracy rates of 96.38% and 97.33%, respectively, using CNN-based approaches for lung cancer diagnosis, whereas the proposed method, combining CNN and VGG19, outperforms existing methods with an accuracy rate of 99.04% for lung and colon cancer diagnosis.

**Table 8:** Comparative analysis of proposed research study and previous studies (H-Histopathological)

Author	Cancer type	Image Type	Classifier	Precision	Recall	F1 Score	Accuracy
Proposed method [54]	Lung, colon	H	CNN + VGG19	98.01	98.03	98.9	99.04
Masud et al. [55]	Lung, colon	H	CNN	96.33	96.39	96.37	96.38
Kumar et al. [56]	Lung, colon	H	CNN	98.60	96.60	96.63	98.50
Mangal et al. [57]	Lung	H	CNN	97.89	–	–	–
Liang et al. [58]	Lung	H	MFF-CNN	96	–	–	–
Bukhari et al. [59]	colon	H	ResNet-50	93.91	94.74	96.77	96.27
Shandilya et al. [52]	Lung	H	CAD, CNN	98.67	–	–	–
Sarwinda et al. [60]	colon	H	DenseNet, KNN	98.53	–	–	–
Hatuwal et al. [61]	Lung	H	CNN	97.2	97.33	97.33	97.33

## 5 Conclusion and Future Research Directions

This study aims to develop an automated detection and classification system for lung and colon cancer images to localize the cells accurately. It employs transfer learning-based feature extraction. The proposed method combines CNN with VGG19 to enhance performance. TensorFlow with Keras API is applied on Google Laboratory to evaluate performance metrics such as precision, recall specificity, F1 score, and accuracy. The proposed system, using the fusion features of the VGG-19 model and handcrafted features, achieved a precision of 98%, recall of 98.64%, and accuracy of 99.04% for early diagnosis of the LC25000 dataset images.

Although this research provides valuable insights into the classification of lung and colon cancer, it has several limitations and warrants consideration; firstly, the dataset's properties, including size, quality, and diversity, can significantly impact the efficiency of the models. This study recommends using larger and more diverse datasets, potentially integrating data from multiple sources to enhance model generalization and robustness to alleviate these constraints. In addition, it focuses only on image-based classification, ignoring potential interaction with other modalities such as genomic, clinical, or radiological data. Future research should explore multimodal approaches to improve classification accuracy, adaptability, and patient outcomes. Integrating diverse data sources can uncover complex patterns and relationships, leading to more accurate diagnoses and personalized treatment plans. In addition, this research employs explainable (XAI) techniques to enhance model interpretability, which remains challenging, particularly in complex medical domains. Further research is essential to develop more interpretable models and refine existing XAI methods, providing deep insights into model decision-making processes and facilitating trust in AI-driven diagnostics. In addition, the study concentrates on two types of cancer: lung and colon. Expanding the proposed approach to encompass additional forms of cancer will significantly enhance its relevance and impact in oncology; investigating the model transferability across diverse healthcare settings, patient demographics, and cancer

types is critical for real-world deployment and broad applicability. It can further advance the accuracy, interpretability, adaptability, and clinical utility of the models, ultimately improving patient outcomes and transforming cancer diagnosis and treatment by addressing these limitations and exploring new avenues of research.

**Acknowledgement:** Not applicable.

**Funding Statement:** The authors received no specific funding for this study.

**Author Contributions:** The authors confirm their contribution to the paper as follows: Conceptualization & Design: Majdi Rawashdeh, Meryem Abouali, and Muath A. Obaidat. Data Collection: Majdi Rawashdeh and Dhia Eddine Salhi. Methodology: Majdi Rawashdeh, Meryem Abouali, and Muath A. Obaidat. Formal Analysis: Majdi Rawashdeh and Kutub Thakur. Supervision: Majdi Rawashdeh. Writing: Majdi Rawashdeh, Muath A. Obaidat, Meryem Abouali, Dhia Eddine Salhi, and Kutub Thakur. Review and Editing: Majdi Rawashdeh and Muath A. Obaidat. Discussion: Majdi Rawashdeh, Muath A. Obaidat, Meryem Abouali, Dhia Eddine Salhi, and Kutub Thakur. All authors reviewed the results and approved the final version of the manuscript.

**Availability of Data and Materials:** The data is available upon request.

**Ethics Approval:** Not applicable.

**Conflicts of Interest:** The authors declare no conflicts of interest to report regarding the present study.

## References

1. Siegel RL, Miller KD, Fuchs HE, Jemal A. Cancer statistics, 2021. *CA A Cancer J Clinicians*. 2021;71(1):7–33. doi:10.3322/caac.21654.
2. Ghasemi S, Akbarpour S, Farzan A, Ali Jabraeil Jamali M. Automatic pulmonary nodule detection on computed tomography images using novel deep learning. *Multimed Tools Appl*. 2024;83(18):55147–73. doi:10.1007/s11042-023-17502-3.
3. Trung NT, Trinh DH, Trung NL, Luong M. Low-dose CT image denoising using deep convolutional neural networks with extended receptive fields. *Signal Image Video Processing*. 2022;16(7):1963–71. doi:10.1007/s11760-022-02157-8.
4. Wang Q, Zuo M. A novel variational optimization model for medical CT and MR image fusion. *Signal Image Video Process*. 2023;17(1):183–90. doi:10.1007/s11760-022-02220-4.
5. Jiang H, Ma H, Qian W, Gao M, Li Y. An automatic detection system of lung nodule based on multigroup patch-based deep learning network. *IEEE J Biomed Health Inform*. 2017;22(4):1227–37. doi:10.1109/JBHI.2017.2725903.
6. Gupta P, Shukla AP. Improving accuracy of lung nodule classification using AlexNet model. In: 2021 International Conference on Innovative Computing, Intelligent Communication and Smart Electrical Systems (ICSES); 2021 Sep 24–25; Chennai, India: IEEE; 2021. p. 1–6. doi:10.1109/ICSES52305.2021.9633903.
7. Khehrah N, Farid MS, Bilal S, Khan MH. Lung nodule detection in CT images using statistical and shape-based features. *J Imaging*. 2020;6(2):6. doi:10.3390/jimaging6020006.
8. Xie Y, Zhang J, Xia Y, Fulham M, Zhang Y. Fusing texture, shape and deep model-learned information at decision level for automated classification of lung nodules on chest CT. *Inf Fusion*. 2018;42(2):102–10. doi:10.1016/j.inffus.2017.10.005.
9. Nasser IM, Abu-Naser SS. Lung cancer detection using artificial neural network. *Int J Eng Inf Syst*. 2019;3(3):17–23.
10. Mohandass G, Hari Krishnan G, Selvaraj D, Sridhathan C. Lung cancer classification using optimized attention-based convolutional neural network with DenseNet-201 transfer learning model on CT image. *Biomed Signal Process Contr*. 2024;95(3):106330. doi:10.1016/j.bspc.2024.106330.
11. LeCun Y, Bottou L, Bengio Y, Haffner P. Gradient-based learning applied to document recognition. *Proc IEEE*. 1998;86(11):2278–324. doi:10.1109/5.726791.



12. Zhang S, Sun F, Wang N, Zhang C, Yu Q, Zhang M, et al. Computer-aided diagnosis (CAD) of pulmonary nodule of thoracic CT image using transfer learning. *J Digit Imaging*. 2019;32(6):995–1007. doi:10.1007/s10278-019-00204-4.
13. Zhao X, Liu L, Qi S, Teng Y, Li J, Qian W. Agile convolutional neural network for pulmonary nodule classification using CT images. *Int J Comput Assist Radiol Surg*. 2018;13(4):585–95. doi:10.1007/s11548-017-1696-0.
14. Sharma G, Jadon VK. Classification of image with convolutional neural network and TensorFlow on CIFAR-10 dataset. In: *International Conference on Women Researchers in Electronics and Computing*; 2023; Singapore: Springer Nature.
15. Polat H, Danaei Mehr H. Classification of pulmonary CT images by using hybrid 3D-deep convolutional neural network architecture. *Appl Sci*. 2019;9(5):940. doi:10.3390/app9050940.
16. Ali AS, Iqbal MM, Khan AH, Hameed N, Bibi S. Lung cancer detection using convolutional neural networks from computed tomography images. *J Comput Biomed Inform*. 2023;6(1):133–43.
17. Lin CJ, Li YC. Lung nodule classification using taguchi-based convolutional neural networks for computer tomography images. *Electronics*. 2020;9(7):1066. doi:10.3390/electronics9071066.
18. Al-Yasriy HF, AL-Husieny MS, Mohsen FY, Khalil EA, Hassan ZS. Diagnosis of lung cancer based on CT scans using CNN. *IOP Conf Ser: Mater Sci Eng*. 2020;928(2):022035. doi:10.1088/1757-899X/928/2/022035.
19. Patil NC. Lung cancer detection using CNN VGG19+ model. *Jes*. 2024;20(3):541–50. doi:10.52783/jes.2981.
20. Elnakib A, Amer HM, Abou-Chadi FEZ. Early lung cancer detection using deep learning optimization. *Int J Onl Eng*. 2020;16(6):82–94. doi:10.3991/ijoe.v16i06.13657.
21. Geng L, Zhang S, Tong J, Xiao Z. Lung segmentation method with dilated convolution based on VGG-16 network. *Comput Assist Surg*. 2019;24(sup2):27–33. doi:10.1080/24699322.2019.1649071.
22. Pang S, Meng F, Wang X, Wang J, Song T, Wang X, et al. VGG16-T: a novel deep convolutional neural network with boosting to identify pathological type of lung cancer in early stage by CT images. *Int J Comput Intell Syst*. 2020;13(1):771–80. doi:10.2991/ijcis.d.200608.001.
23. Agarwal A, Patni K, Rajeswari D. Lung cancer detection and classification based on alexnet CNN. In: *Proceedings of the 2021 6th International Conference on Communication and Electronics Systems (ICCES)*; 2021 Jul 8–10; Coimbatre, India. p. 1390–7.
24. Saha A, Ganie SM, Pramanik PKD, Yadav RK, Mallik S, Zhao Z. VER-Net: a hybrid transfer learning model for lung cancer detection using CT scan images. *BMC Med Imaging*. 2024;24(1):120. doi:10.1186/s12880-024-01238-z.
25. Shin HC, Roth HR, Gao M, Lu L, Xu Z, Nogues I, et al. Deep convolutional neural networks for computer-aided detection: cnn architectures, dataset characteristics and transfer learning. *IEEE Trans Med Imaging*. 2016;35(5):1285–98. doi:10.1109/TMI.2016.2528162.
26. Zheng G, Han G, Soomro NQ. An inception module CNN classifiers fusion method on pulmonary nodule diagnosis by signs. *Tsinghua Sci Technol*. 2020;25(3):368–83. doi:10.26599/TST.2019.9010010.
27. Lin H, Tao S, Song S, Liu H. An improved yolov3 algorithm for pulmonary nodule detection. In: *2021 IEEE 4th Advanced Information Management, Communicates, Electronic and Automation Control Conference (IMCEC)*; 2021 Jun 18–20; Chongqing, China: IEEE; 2021. p. 1068–72. doi:10.1109/imcec51613.2021.9482291.
28. Bu Z, Zhang X, Lu J, Lao H, Liang C, Xu X, et al. Lung nodule detection based on YOLOv3 deep learning with limited datasets. *Mol Cell Biomech*. 2022;19(1):17–28. doi:10.32604/mcb.2022.018318.
29. Zhang X, Lee VCS, Rong J, Liu F, Kong H. Multi-channel convolutional neural network architectures for thyroid cancer detection. *PLoS One*. 2022;17(1):e0262128. doi:10.1371/journal.pone.0262128.
30. Leo M, Cacagni P, Signore L, Benincasa G, Laukkanen MO, Distanti C. Improving colon carcinoma grading by advanced CNN models. In: *International Conference on Image Analysis and Processing*; 2022; Cham, Switzerland: Springer. p. 233–44.
31. Lanjewar M, Panchbhaj KG, Panem C. Lung cancer detection from CT scans using modified DenseNet with feature selection methods and ML classifiers. *Expert Syst Appl*. 2023;224(8):119961. doi:10.1016/j.eswa.2023.119961.
32. Maurya SP, Sisodia PS, Mishra R, Singh DP. Performance of machine learning algorithms for lung cancer prediction: a comparative approach. *Sci Rep*. 2024;14(1):18562. doi:10.1038/s41598-024-58345-8.

33. Hossain N, Anjum N, Alam M, Rahman MH, Taluckder MS, et al. Performance of machine learning algorithms for lung cancer prediction: a comparative study. *Int J Med Sci Public Health Res.* 2024;5(11):41–55. doi:10.37547/ijmsphr/Volume05Issue11-05.
34. Javed R, Abbas T, Khan AH, Daud A, Bukhari A, Alharbey R. Deep learning for lungs cancer detection: a review. *Artif Intell Rev.* 2024;57(8):197. doi:10.1007/s10462-024-10807-1.
35. Liz-López H, de Sojo-Hernández ÁA, D'Antonio-Maceiras S, Díaz-Martínez MA, Camacho D. Deep learning innovations in the detection of lung cancer: advances, trends, and open challenges. *Cogn Comput.* 2025;17(2):67. doi:10.1007/s12559-025-10408-2.
36. Perumal V, Narayanan V, Rajasekar SJS. Detection of COVID-19 using CXR and CT images using Transfer Learning and Haralick features. *Appl Intell.* 2021;51(1):341–58. doi:10.1007/s10489-020-01831-z.
37. Li L, Qin L, Xu Z, Yin Y, Wang X, Kong B, et al. Artificial intelligence distinguishes COVID-19 from community acquired pneumonia on chest CT. *Radiology.* 2020;296(2):65–71.
38. Wang S, Kang B, Ma J, Zeng X, Xiao M, Guo J, et al. A deep learning algorithm using CT images to screen for *Corona* virus disease (COVID-19). *Eur Radiol.* 2021;31(8):6096–104. doi:10.1007/s00330-021-07715-1.
39. Xu X, Jiang X, Ma C, Du P, Li X, Lv S, et al. A deep learning system to screen novel coronavirus disease 2019 pneumonia. *Engineering.* 2020;6(10):1122–9. doi:10.1016/j.eng.2020.04.010.
40. Song Y, Zheng S, Li L, Zhang X, Zhang X, Huang Z, et al. Deep learning enables accurate diagnosis of novel coronavirus (COVID-19) with CT images. *IEEE/ACM Trans Comput Biol Bioinform.* 2021 Nov 1–Dec;18(6):2775–80. doi:10.1109/TCBB.2021.3065361.
41. Wang B, Jin S, Yan Q, Xu H, Luo C, Wei L, et al. AI-assisted CT imaging analysis for COVID-19 screening: building and deploying a medical AI system. *Appl Soft Comput.* 2021;98(10223):106897. doi:10.1016/j.asoc.2020.106897.
42. Maghdid HS, Asaad AT, Ghafoor KZ, Sadiq AS, Khan MK. Diagnosing COVID19 pneumonia from X-ray and CT images using deep learning and transfer learning algorithms. arXiv:2004.00038. 2020.
43. Zhang J, Xie Y, Li Y, Shen C, Xia Y. COVID-19 screening on chest X-ray images using deep learning based anomaly detection. arXiv:2003.12338. 2020.
44. Khalifa NEM, Taha MHN, Hassanien AE, Elghamrawy S. Detection of coronavirus (COVID-19) associated pneumonia based on generative adversarial networks and a fine-tuned deep transfer learning model using chest X-ray dataset. arXiv:2004.01184. 2020.
45. Hammoudi K, Benhabiles H, Melkemi M, Dornaika F, Arganda-Carreras I, Collard D, et al. Deep learning on chest X-ray images to detect and evaluate pneumonia cases at the era of COVID-19. arXiv:2004.03399. 2020.
46. Farooq M, Hafeez A. COVID-ResNet: a deep learning framework for screening of COVID19 from radiographs. arXiv:2003.14395. 2020.
47. Sultana Z, Foysal M, Islam S, Al Foysal A. Lung cancer detection and classification from chest CT images using an ensemble deep learning approach. In: 2024 6th International Conference on Electrical Engineering and Information & Communication Technology (ICEEICT); 2024 May 2–4; Dhaka, Bangladesh: IEEE; 2024. p. 364–9. doi:10.1109/ICEEICT62016.2024.10534468.
48. Borkowski A, Bui M, Thomas L, Wilson C, DeLand L, Mastorides S. Lung and colon cancer histopathological image dataset (lc25000). arXiv:1912.12142. 2019.
49. Lu Y, Liang H, Shi S, Fu X. Lung cancer detection using a dilated CNN with VGG16. In: 2021 4th International Conference on Signal Processing and Machine Learning; 2021; Beijing, China: ACM. p. 45–51. doi:10.1145/3483207.3483215.
50. Bhattacharyya N, Satish AS. A study of accuracy in detection of lung cancer through CNN models. *Des Eng.* 2021;9:1250–70.
51. Ramana K, Kumar MR, Sreenivasulu K, Gadekallu TR, Bhatia S, Agarwal P, et al. Early prediction of lung cancers using deep saliency capsule and pre-trained deep learning frameworks. *Front Oncol.* 2022;12:886739. doi:10.3389/fonc.2022.886739.
52. Shandilya S, Nayak SR. Analysis of lung cancer by using deep neural network. In: *Innovation in Electrical Power Engineering, Communication, and Computing Technology: Proceedings of Second IEPCCCT 2021*; 2022; Singapore: Springer.

53. Abd Al-Ameer AA, Abdulameer Hussien G, Al Ameri HA. Lung cancer detection using image processing and deep learning. *Indones J Electr Eng Comput Sci.* 2022;28(2):987. doi:10.11591/ijeecs.v28.i2.pp987-993.
54. Rawashdeh M, Obaidat MA, Abouali M, Thakur K. A deep learning-driven approach for detecting lung and colon cancer using pre-trained neural networks. In: *2024 IEEE 21st International Conference on Smart Communities: Improving Quality of Life using AI, Robotics and IoT (HONET); 2024 Dec 3–5; Doha, Qatar: IEEE; 2024.* p. 183–8. doi:10.1109/HONET63146.2024.10822988.
55. Masud M, Sikder N, Nahid AA, Bairagi AK, AlZain MA. A machine learning approach to diagnosing lung and colon cancer using a deep learning-based classification framework. *Sensors.* 2021;21(3):748. doi:10.3390/s21030748.
56. Kumar N, Sharma M, Singh VP, Madan C, Mehandia S. An empirical study of handcrafted and dense feature extraction techniques for lung and colon cancer classification from histopathological images. *Biomed Signal Process Contr.* 2022;75(1):103596. doi:10.1016/j.bspc.2022.103596.
57. Mangal S, Chaurasia A, Khajanchi A. Convolution neural networks for diagnosing colon and lung cancer histopathological images. *arXiv:2009.03878.* 2020.
58. Liang M, Ren Z, Yang J, Feng W, Li B. Identification of colon cancer using multi-scale feature fusion convolutional neural network based on shearlet transform. *IEEE Access.* 2020;8:208969–77. doi:10.1109/ACCESS.2020.3038764.
59. Bukhari SUK, Syed A, Bokhari SKA, Hussain SS, Armaghan SU, Shah SSH. The histological diagnosis of colonic adenocarcinoma by applying partial self-supervised learning. *MedRxiv.* 2020. doi:10.1101/2020.08.15.20175760.
60. Sarwinda D, Bustamam A, Paradisa RH, Argyadiva T, Mangunwardoyo W. Analysis of deep feature extraction for colorectal cancer detection. In: *2020 4th International Conference on Informatics and Computational Sciences (ICICoS); 2020 Nov 10–11; Semarang, Indonesia: IEEE; 2020.* p. 1–5. doi:10.1109/icicos51170.2020.9298990.
61. Hatuwal BK, Thapa HC. Lung cancer detection using convolutional neural network on histopathological images. *Int J Comput Trends Technol.* 2020;68(10):21–4. doi:10.14445/22312803/IJCTT-V68I10P104.